YAW STABILIZATION OF LANDING CRAFT

R. J. Hinkle

Supervisor: Prof. M. A. Abkowitz
May 20, 1966

YAW STABILIZATION OF LANDING CRAFT

by
RICHARD JON HINKLE
S.B., UNITED STATES COAST GUARD ACADEMY
(1961)

SUBMITTED IN PARTIAL FULFILLMENT
OF THE REQUIREMENTS FOR THE
DEGREE OF MASTER OF
SCIENCE
at the
MASSACHUSETTS INSTITUTE OF
TECHNOLOGY
JUNE, 1966

Signature of Author...
Department of Naval Architecture and
Marine Engineering, May 20, 1966

Certified by..
Thesis Supervisor

Accepted by...
Chairman, Departmental Committee
on Graduate Students

YAW STABILIZATION OF LANDING CRAFT

RICHARD JON HINKLE

Submitted to the Department of Naval Architecture and Marine Engineering on May 20, 1966 in partial fulfillment of the requirements for the Master of Science degree in Naval Architecture and Marine Engineering.

The purpose of this work was to investigate the application of pump jet propulsion and yaw angle stabilization for a landing craft going through the surf. Linear theory was used throughout the analysis of the control problem. The stability indices and derivatives were determined in part by experiment and the remainder by analytic techniques.

It was found that LCVP landing craft are dynamically unstable without a skeg. Stability could possibly be restored by a feedback control system, but the far more practical solution is to start with a dynamically stable craft. This will provide the craft with a greater margin of stability in all cases.

Although it is felt that the craft can not be satisfactorily used without a skeg, much of the analytic data in Appendix A may be used to cover the case with a skeg. Reference (3) contains the appropriate modifications needed for the changes.

Thesis Supervisor: MARTIN A. ABKOWITZ

Title: Professor of Naval Architecture

TABLE OF CONTENTS

Page

ABSTRACT i

SYMBOLS 1

INTRODUCTION 3

PROCEEDURE 5

RESULTS 12

DISCUSSION OF RESULTS 21

CONCLUSION 27

RECOMMENDATIONS 28

BIBLIOGRAPHY 29

APPENDIX 30

APPENDIX A 31

[illegible]

May, 1966

INDEX OF FIGURES

Page

FIGURE I Block Diagram of Ship 7

FIGURE II Control System 10

FIGURE III Resistance Data 15

FIGURE IV Resistance Plot 16

FIGURE V Experimental Values of Y_v and N_v 17

FIGURE VI Plot of Y_v and N_v 18

FIGURE VII Stability Indices and Derivatives 19

FIGURE VIII Block Diagram of Ship and Control System 20

FIGURE IX Nyquist Criteria Plot 22

FIGURE X Root Locus at 4.5 Knots 23

FIGURE XI Root Locus at 7.5 Knots 24

FIGURE XII Calculations of Stability Indices and Derivatives 33

FIGURE XIII Calculations of Stability Indices and Derivatives 35

FIGURE XIV Calculations of Stability Indices and Derivatives 37

FIGURE XV Calculations of Stability Indices and Derivatives 38

FIGURE XVI Calculations of Stability Indices and Derivatives 39

FIGURE XVII Lamb's Coefficients of Accession 40

FIGURE XVIII Prohaska's Sectional Inertia Coefficients 41

SYMBOLS

B	beam
C_s	2-D lateral added mass coefficient (sectional inertia coefficient)
C_f	frictional resistance coefficient
C_r	residuary resistance coefficient
C_t	total resistance coefficient
ΔC_f	roughness correction to C_f
g	acceleration due to gravity
h	local draft
I_o	moment of inertia of hull
I_a	added moment of inertia of entrained water
k_1	Lamb's coefficient of accession to longitudinal inertia
k_2	Lamb's coefficient of accession to lateral inertia
k'	Lamb's coefficient of accession to rotational inertia
l	length
m_o	mass of hull
m_1	longitudinal added mass
m_2	lateral added mass
m_3	rotational added mass
N	yaw moment
N_F	Froude Number
N_R	Reynolds Number
$r = \dot{\psi}$	yaw angle rate

u_o	velocity of hull center of gravity in the forward direction
s	differential operator
v	velocity of hull C.G. in starboard direction
x	longitudinal distance from L.C.G. to the C.G. of the lateral added mass
x_G	distance to L.C.G. from the reference point for forces, moments, velocities etc.
x_p	Longitudinal distance from L.C.G. to the center of pressure at which the lateral force Y acts (taken as center of area of hull profile)
x_o/l	approximated by half the prismatic coefficient
Y	force in the starboard direction
ρ	mass density of water
ψ	yaw angle
r&v	subscripts meaning partial derivative with respect to r&v respectively
m	subscript meaning maximum value

INTRODUCTION

Landing craft used in amphibious warfare are susceptable to broaching while transiting the surf. The craft, in the surf, is particularly vulnerable because it is in a following sea and also the relative velocity of the water in the vicinity of the rudder is small, making the rudder less effective.

A possible method of reducing this broaching problem is to use a yaw angle control system. By replacing the screw propeller and rudder with a pump jet with a controlled discharge angle, the problem of decreased rudder effectiveness would be eliminated. A pump jet propulsion system of the size required for the craft needs some means of power assist to vector the jet stream for steering. This vectoring system might easily be converted to an automatic steering control system to minimize the yaw angle and eliminate broaching. The economics of war require that in order to be effective the craft must be cheap so the control system must be of relatively simple design and accuate for small periods of time such as transiting a surf line.

The equations of motion for the craft are a pair of linearized second order differential equations relating yaw and sway to the yawing moments and the transverse force. The coefficients for the various terms in these equations were determined by either experiment on a model LCVP or the

analytical approach of Jacobs (2). The current LCVPs are equipped with a skeg for improved dynamic stability and protection of the propeller. The tests run on the model at the towing tank were all conducted without this skeg.

The analysis of the control problem was done using linear control theory. The criteria of stability for the system was either that of Nyquist or by root locus. A model of the system for the analog computer was made, but due to the instability the results are not shown.

PROCEDURE

From the general linearized equations of ship motion of Abkowitz (1) the equations for yaw and sway were obtained by decoupling the equations for the other modes of freedom. The resulting equations are:

$$\overset{b_{11}}{(Y_r - mx_G)}\frac{d^2\psi}{dt^2} + \overset{b_{12}}{(Y_r - mu_o)}\frac{d\psi}{dt} + \overset{b_{13}}{(Y_r - m)}\frac{dv}{dt} + \overset{b_{14}}{Y_v} v = -Y_{rud} - Y_d \qquad (1)$$

$$\underset{b_{21}}{(N_r - I_z)}\frac{d^2\psi}{dt^2} + \underset{b_{22}}{(N_r - mx_G u_o)}\frac{d\psi}{dt} + \underset{b_{23}}{(N_v - mx_G)}\frac{dv}{dt} + \underset{b_{24}}{N_v} v = -N_{rud} - N_d \qquad (2)$$

where Y_{rud} and N_{rud} stand for the forces or moments caused by the steering device and the subscript d for the disturbance. Noting that any force can be resolved into a force and a moment at some other location, the force, due to deflecting the pump jet, will become the Y_{rud} and N_{rud} at the reference position for the equations. N_{rud} is simply Y_{rud} multiplied by the distance k between its place of application and the reference point. A similar treatment applies to disturbance forces and moments. Reducing the pair of simultaneous equations to one equation in ψ and Y force we have:

$$\psi\Big[(b_{21}b_{13} - b_{11}b_{23})s^3 + (b_{14}b_{21} + b_{13}b_{22} - b_{24}b_{14} - b_{23}b_{12})s^2 +$$

$$(b_{14}b_{22} - b_{24}b_{12})s\Big] = Y_{rud}\Big[(b_{23} - kb_{13})s + (b_{24} - kb_{14})\Big] + Y_d\Big[(b_{23} - k'b_{13})s + (b_{24} - k'b_{14})\Big]$$

The block diagram representation of the ship is shown in figure I.

The determination of the stability derivatives was done by experiment where the necessary equipment was available and the remaining derivatives evaluated analytically. The evaluation of N_v was done by towing the model in the tank at a small yaw angle and measuring the moment. The moment was measured by constructing a heave rod with the lower eight inches machined round and instrumenting the round portion with a full bridge of strain gauges. The full bridge array allowed the measurement of torque without any effect due to the bending moment in the bar. The output of this dynamometer was averaged by an integrator to obtain the result. Measurement of Y_v was accomplished at the same time by mounting the thrust block athwartships in the model to measure the force in the Y direction. Runs were made at three separate yaw angles at each of four different speeds. These measurements were made at the longitudinal center of gravity in order to have several terms drop out of the equations. The remaining stability derivatives were calculated using the method set forth in *Estimation of Stability Derivatives [illegible] Various Ship Forms, and Comparison With Experimental Results* by Jacobs. This method employs a strip theory technique with lateral added mass coefficient along with Lamb's coefficients of accession to inertia and hydrofoil theory.

The use of pump jet propulsion introduces an additional

FIGURE I

Block Diagram of Ship

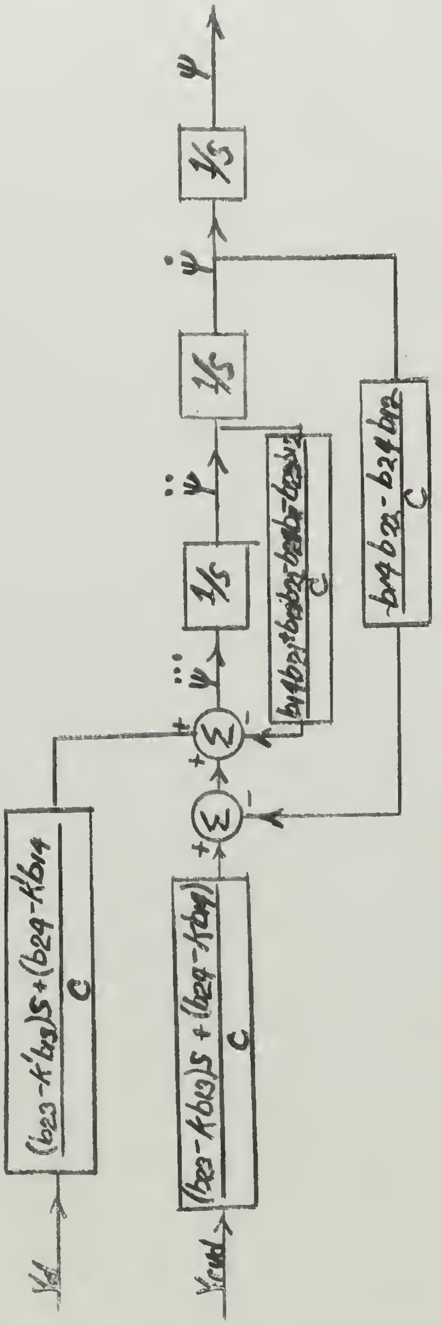

$C = b_{21}b_{13} - b_{11}b_{23}$

factor in both the Y_r and N_r derivatives. Due to the relatively high velocity of the water jet, a rotational momentum change force become significant. The force derivative is equal to twice the mass of the water in the duct times the velocity of the water jet. The moment derivative is derived by applying this force half way down the longitudinal length of the discharge duct. For purposes of calculations a ten foot duct with a six inch diameter was assumed. The thrust of the pump jet was determined by scaling up model resistance data obtained in the towing tank. An attempt was made to gather resistance data for the model in a surf but the waves would not break for a long enough distance to gather any data.

Because pump jet propulsion was employed, the skeg was not needed for protection of the propeller and was not on the model during the tests. The elimination of the skeg made the model dynamically unstable in straight line motion.

The automatic control system was chosen to be one of few parts. The quantities ψ and $\dot{\psi}$ are measured by a free gyro and a rate gyro. It may be acceptable to have accuracy [illegible] periods of time such as when going through the surf. In this case the measurement of ψ can be accomplished by using the gyro as a free gyroscope rather than as a null device. If the gyroscope is free, some means of sensing its position without applying much torque, such as a differential transformer, will have to be used to avoid unwanted precession. The values of ψ and $\dot{\psi}$ times their appropriate gains are summed and compared with the rudder angle and

the difference applied to a push pull amplifier. The output of the amplifier is a solenoid shown in figure II. By keeping the magnetic field in the solenoid large enough the plunger will become magnetically saturated. The force exerted by the coils on the plunger will then become directly proportional to the current. The position of the plunger is used to control an underlapped spool valve of the constant pressure hydraulic system. The reaction of the spool valve as a spring and damper were considered so that this portion of the system could be critically damped. This was done to help reduce the high frequency oscillations of the vectoring duct. The output from this four way valve drives the rams that position the jet vectoring duct.

The removal of the skeg made the craft dynamically unstable. The next step was to investigate what could be done by the control system to restore the dynamical stability. First, the effects of control, proportional only to yaw angle, was investigated. It was shown by the Nyquist Stability Criteria that, at the speed chosen for investigation, no amount of gain would suffice for stabilization. Proceeding to a control proportional to yaw angle and yaw rate again, it could be shown that the system would be ineffective. Using a root locus plot, it can be seen that the right most two poles would continue to stay on the right half plane for all values of gain. By studing the root locus further, it can be seen that a system proportional to yaw plus the first and second derivatives would be the minimum requirement to produce

FIGURE II

Control system

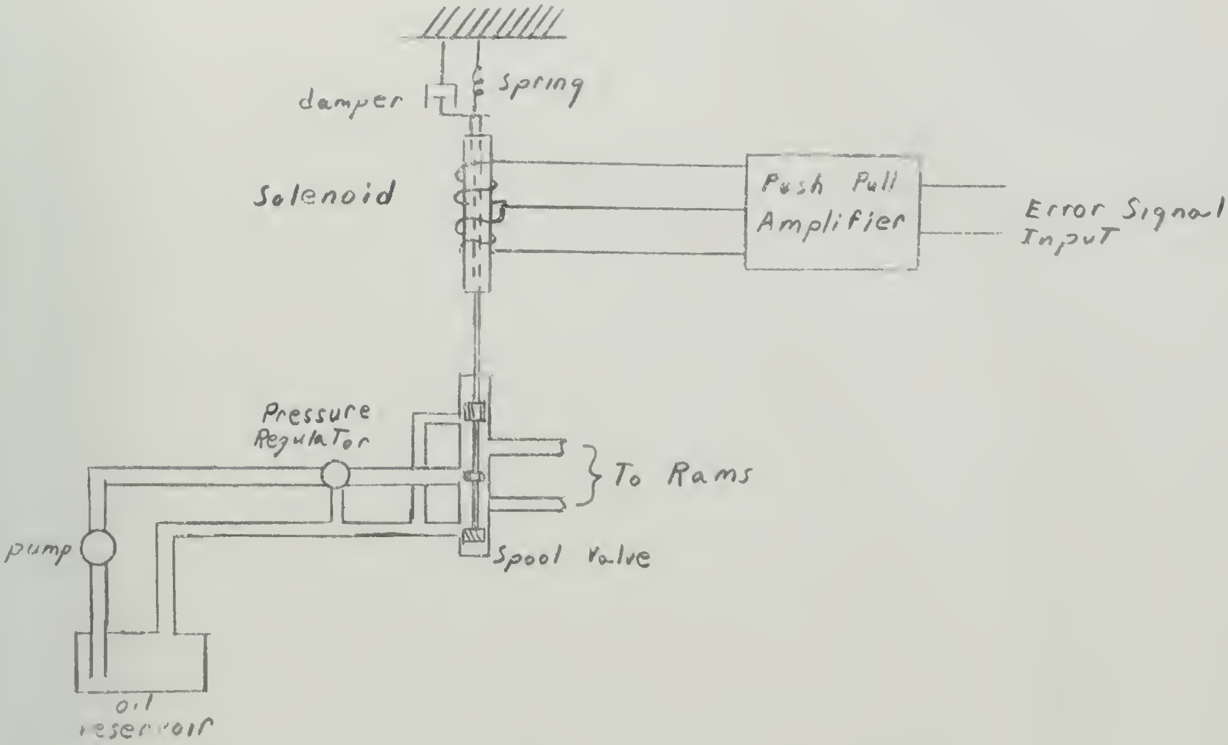

a dynamically stable craft by adding two complex conjugate zeros to the root locus through the use of appropriate feed back gains, the unstable roots could be brought over to the left half plane. The design of such a system was dismissed however. Rydill (3) claims that such systems are not satisfactory due to excessive high frequency oscillations of the steering device. Also, the expense of the extra equipment needed for the control could be eliminated by reinstalling the skeg and making the craft dynamically stable to begin with.

RESULTS

The results of this investigation were based on the following assumptions regarding the design of the system:

a. longitudinal length of jet duct is 10 feet

b. jet duct diameter is 6 inches

c. Y force from deflected jet acts 15.94 feet from L.C.G.

d. density of the hydraulic fluid 57 lbs/ft^3

e. mass of spool valve and plunger is $6.88 \times 10^{3}\ \frac{\text{lbs-sec}^2}{\text{in}}$

f. discharge coefficients for spool valve [illegible]

g. width of spool valve ports are 0.75 inches

h. the rams that drive the jet vectoring conduit are 1 square inch in area and are located 6 inches from the swivel, therefore the discharge angle is equal to the ram travel in inches over 6

i. supply pressure is constant at 1000 psi

j. the radius of gyration equals one forth the length

The thrust to be developed must equal the resistance of the craft for constant velocity operation. The model was tested in the towing tank and the model resistance data and scaled up results are tabulated in figure III. A plot of the full scale resistance is shown in figure IV.

The qualities Y_v and N_v were found experimentally in the towing tank. The three yaw angles used during the testing were 3.12°, 5.92°, and 9.30° and the model speeds varied from 1.3 knots

to 2.9 knots. This corresponded to speeds between 4.75 and 10.5 knots for the full scale craft. A table of the experimental data is presented in figure V. The data was non-dementionalized by dividing forces by $\rho/_2\, u^2 l^2$ and moments by $\rho/_2\, u^2 l^3$. Both N_v and Y_v were found to be dependent on Froude Number as is shown by the plot in figure VI. The variation of yaw angle due to the twisting of the rod was computed for the largest torque experienced and the effect was found to be insignificant.

The data for the remainder of the stability derivatives and indices was computed by the method outlined in reference 2. The method of non-dementionalizing used here was to divide forces by $u/_l$. The length used in all calculations here was that of the waterline 32.367 feet. The actual computations of these derivatives and indices are contained in appendix A.

The value of stability indices, derivatives, and resistance for speeds of 4 and 7.5 knots are listed in figure V11.

The spool valve is an underlapped four way valves with ports 0.75 inches wide and discharge coefficients of 0.7 at each port. The equations for flow rate for such a valve is that $j=\frac{2k}{A}\sqrt{P_s/2}\,x$ where j is ram rate, X is spool value displacement, P_s is supply pressure, k is the product of discharge coefficient, port width and the square root of two times the acceleration of gravity divided by the mass of the density of the hydraulic fluid. $(k=CW\sqrt{2g/\rho}$ This equation gives $j=3600x$ for this system. The spring reaction force of the valve is given by the equqtion:

$k=2 \times \text{discharge coefficient} \times \text{port width} \times P_s \times \cos 69°$

or $k=2 \times 0.7 \times 0.75 \times 10^3 \times 0.358 = 376 \ \text{lb}/\text{in.}$

The damping reaction of the spool valve is expressed by the equation:

$C=\text{discharge coefficient} \times \text{port width} \times \sqrt{\frac{\rho P_s}{g}} \times L$

where L is the difference between distance from supply port to load port and load port to drain port. With L equal to 2, the value of C is $0.7 \times 0.75 \times 0.293 \times 2 = 0.308 \ \frac{\text{lbs-sec}}{\text{in}}$

By using a spring with a constant of 24 $\frac{\text{lbs}}{\text{in}}$ to center the plunger, the total spring constant becomes 400 $\frac{\text{lbs}}{\text{in}}$. The plunger-spool valve combination is assumed to have a mass of $6.88 \times 10^{-3} \ \frac{\text{lbs-sec}^2}{\text{in}}$

To critically damp this system, a damping constant of $3.32 \frac{\text{lbs-sec}}{\text{in}}$ is needed. An additional damper with a constant of $3.01 \frac{\text{lbs-sec}}{\text{in}}$ would be needed to critically damp the system.

The combined control system and ship block diagram for speeds of 4 and 7.5 knots is illustrated in figures VIII.

FIGURE III

RESISTANCE DATA

v_{model} KTS	$v/\sqrt{l}$	N_R	Resistance lbs	C_t	C_f	C_r
0.608	0.288	4.33×10^5	0.05	0.00974	5.209×10^3	4.53×10^{-3}
1.116	0.528	7.91×10^5	0.1575	0.00914	4.615×10^3	4.52×10^{-3}
1.489	0.705	1.061×10^4	0.283	0.00924	4.363×10^3	4.88×10^{-3}
2.016	0.954	1.428×10^4	0.668	0.01012	4.119×10^3	6.00×10^{-3}
2.467	1.168	1.750×10^4	1.293	0.01533	3.969×10^3	1.116×10^{-2}
2.978	1.408	2.115×10^4	2.413	0.01960	3.831×10^3	1.577×10^{-2}
3.219	1.522	2.282×10^4	3.593	0.02515	3.779×10^3	2.137×10^{-2}

v_{ship} KTS	$v/\sqrt{l}$	N_R	$C_f + \Delta C_f$	C_t	Resistance lbs
1.718	0.288	8.07×10^6	3.439×10^{-3}	7.97×10^{-3}	21.25
3.15	0.528	1.43×10^7	3.170×10^{-3}	7.69×10^{-3}	69.1
4.2	0.705	1.97×10^7	3.035×10^{-3}	7.92×10^{-3}	126.4
5.68	0.954	2.67×10^7	2.913×10^{-3}	8.91×10^{-3}	260.5
6.98	1.168	3.275×10^7	2.837×10^{-3}	1.400×10^{-2}	616
8.40	1.408	3.94×10^7	2.771×10^{-3}	1.854×10^{-2}	1182
9.09	1.522	4.26×10^7	2.743×10^{-3}	2.411×10^{-2}	1807

Figure IV

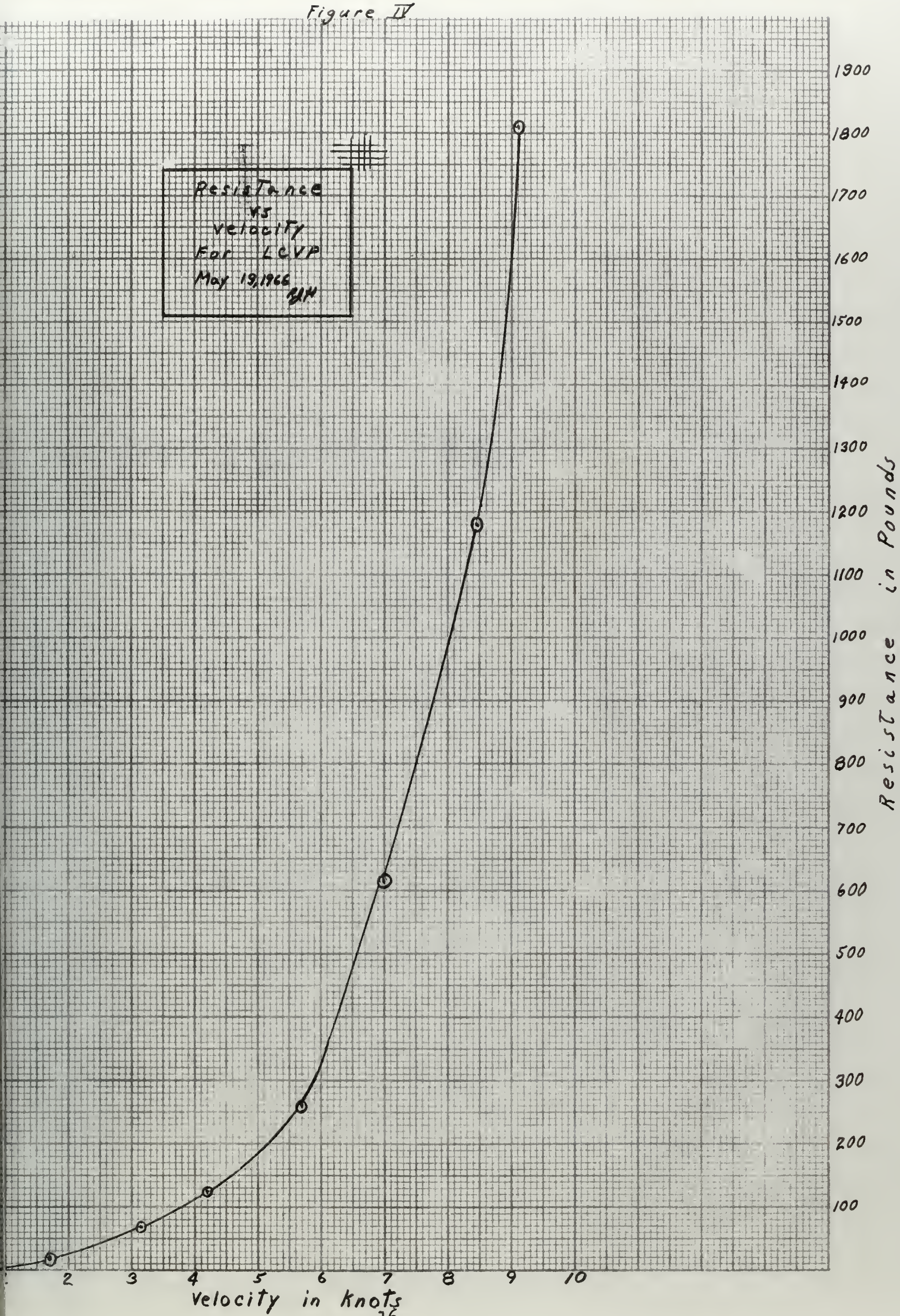
Resistance
vs
velocity
For LCVP
May 19, 1966
1900
1800
1700
1600
1500
1400
1300
1200
1100
1000
900
800
700
600
500
400
300
200
100
Resistance in Pounds
2
3
4
5
6
7
8
9
10
Velocity in knots

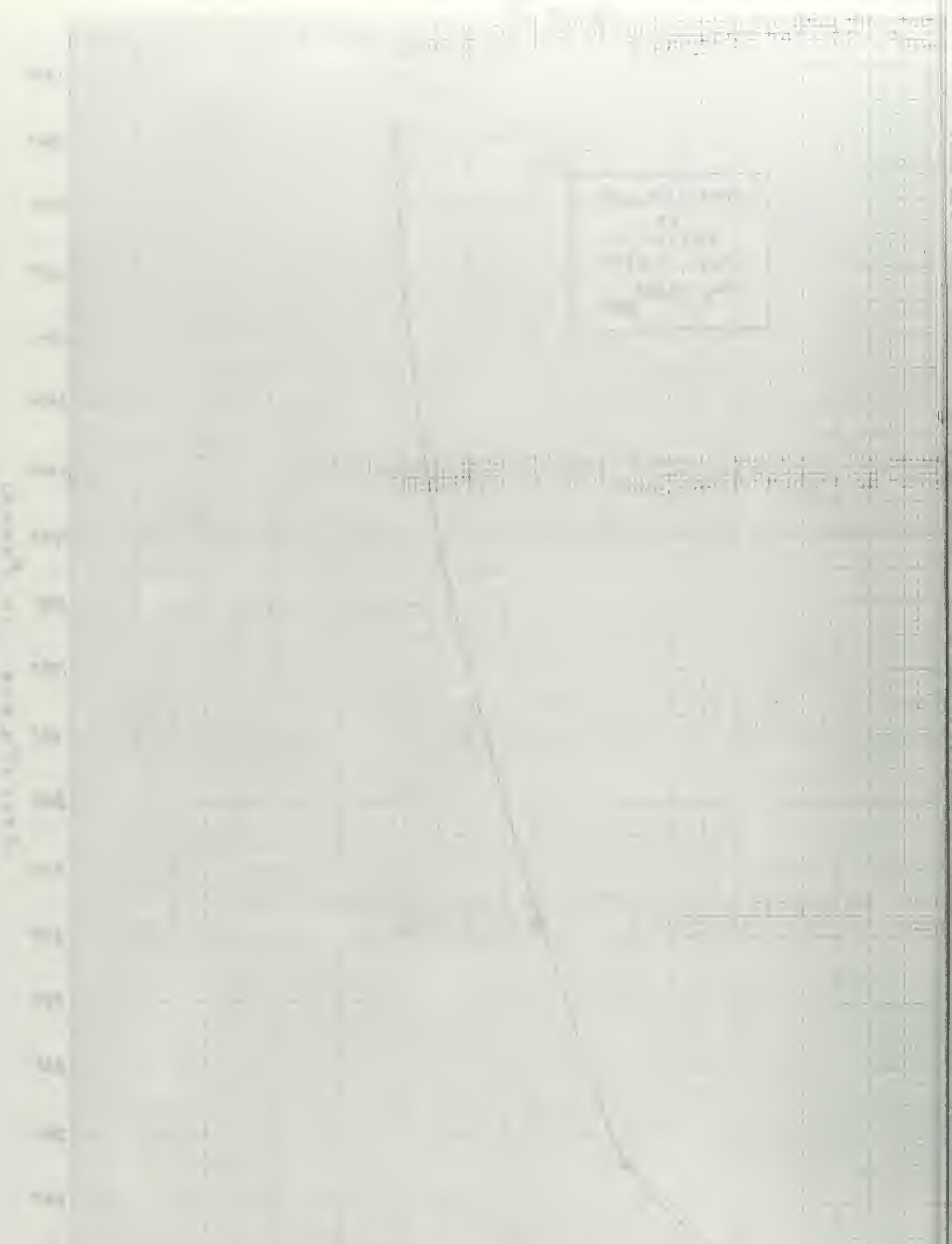

FIGURE V

Experimental Values of Y_v and N_v

$\psi = 3.12°$

U fps	Y lbs	N in lbs	Y'	N'
2.27	0.0613	2.3	6.37×10^{-4}	4.32×10^{-4}
2.27	0.0580	2.03	5.88×10^{-4}	3.81×10^{-4}
3.03	0.0833	3.48	4.72×10^{-4}	3.67×10^{-4}
4.17	0.1868	5.15	5.43×10^{-4}	2.875×10^{-4}
		$\psi = 5.92°$		
2.27	0.1162	3.70	1.173×10^{-3}	6.95×10^{-4}
3.01	0.1186	5.18	6.80×10^{-4}	5.53×10^{-4}
3.03	0.1035	4.75	5.86×10^{-4}	5.00×10^{-4}
4.17	0.4166	8.40	1.25×10^{-3}	4.68×10^{-4}
4.54	0.5307	10.40	1.341×10^{-3}	4.89×10^{-4}
		$\psi = 9.30°$		
2.055	0.1414	2.73	1.749×10^{-3}	6.26×10^{-4}
2.17	0.1818	3.75	1.83×10^{-3}	7.04×10^{-4}
3.03	0.3404	6.30	1.93×10^{-3}	6.64×10^{-4}
4.17	0.7405	12.10	2.22×10^{-3}	6.74×10^{-4}
5.03	1.2020	20.40	2.47×10^{-3}	7.80×10^{-4}

Figure VI

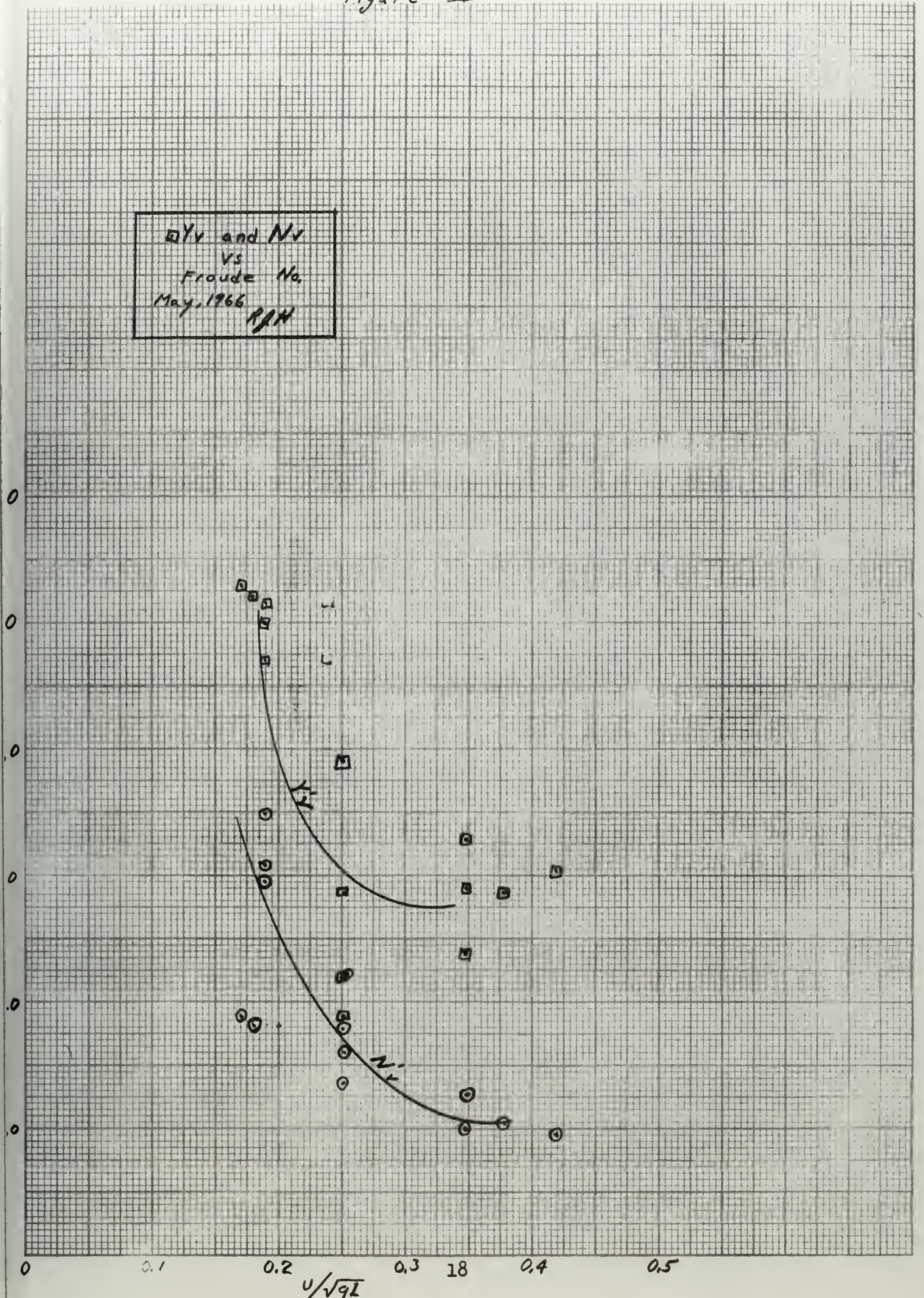
□Yv and Nv
vs
Froude No.
May, 1966
RJH
Y'v
N'v
0
.0
0
.0
0
.0
0
0.1
0.2
0.3
0.4
0.5
U/√gL

FIGURE VII

STABILITIES INDICES AND DERIVATIVES

Speed	4.0	7.5
$Y_{\dot{r}}$	-111.5	-111.5
$Y_{\dot{v}}$	-393.5	-393.5
Y_r	-5,230.0	-9,800.0
Y_v	-94.0	-210.5
$N_{\dot{r}}$	-18,890.0	-18,890.0
$N_{\dot{v}}$	-111.5	-111.5
N_r	-670.0	-1,258.0
N_v	-2855.0	-2,765.0
I	46,700.0	46,700.0
m	2,765.0	2,765.0
Coriolus Force	275.5 r	1,602.0 r
Coriolus Moment	-2,880.0 r	-16,750.0 r
Resistance	115.0	800.0

[illegible]

[illegible]

[illegible]	[illegible]	[illegible]
[illegible]	[illegible]	[illegible]
[illegible]	[illegible]	[illegible]
[illegible]	[illegible]	[illegible]
[illegible]	[illegible]	[illegible]
[illegible]	[illegible]	[illegible]
[illegible]	[illegible]	[illegible]
[illegible]	[illegible]	[illegible]
[illegible]	[illegible]	[illegible]
[illegible]	[illegible]	[illegible]
[illegible]	[illegible]	[illegible]
[illegible]	[illegible]	[illegible]
[illegible]	[illegible]	[illegible]
[illegible]	[illegible]	[illegible]

FIGURE VIII

Block Diagram of Ship and Control System

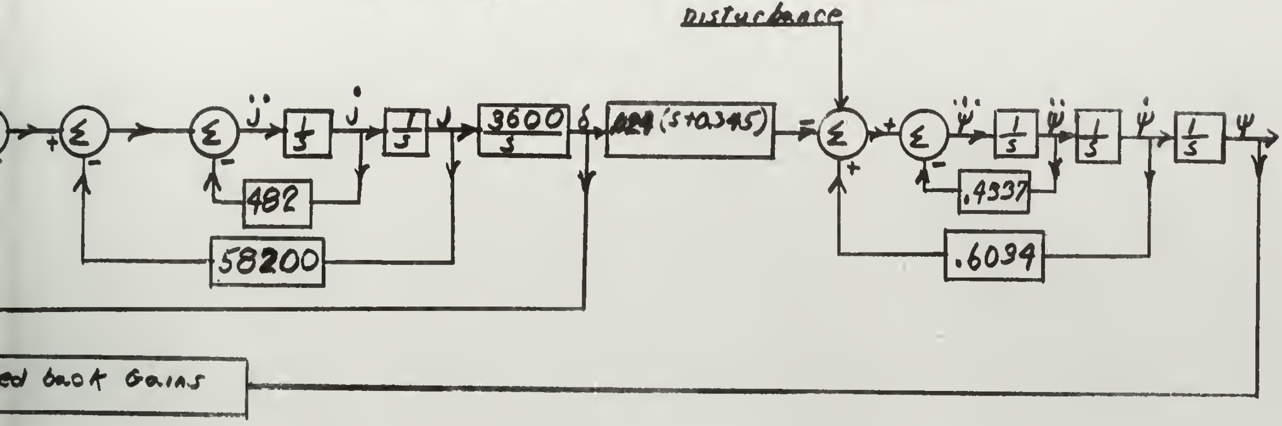

7.5 knots

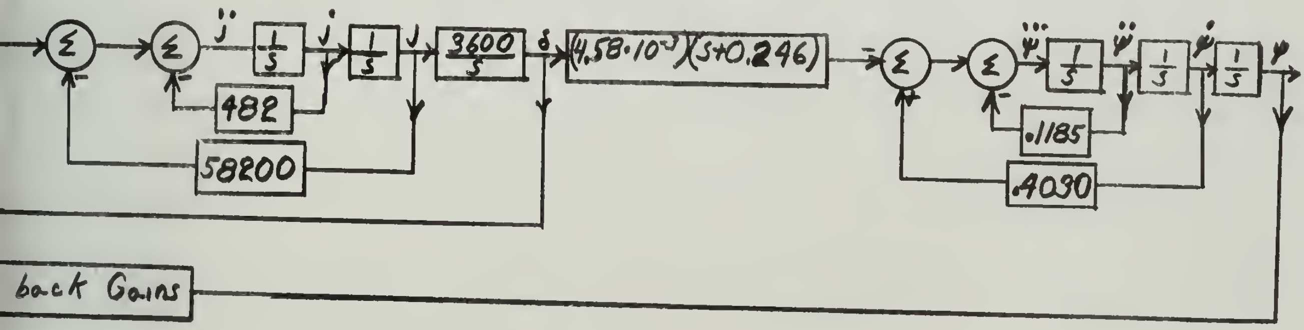

4.0 knots

DISCUSSION OF RESULTS

The instability of the system with control proportional only to yaw angle is shown in figure IX, a Nyquist Stability Criteria plot at 7.5 knots. There is one pole of the open loop transfer function in the right half plane. For unity gain in the control system, there are no encirclements of the minus one point, therefore there will be one root in the right half plane of the closed loop transfer function. By increasing the gain, the small loop near the origin (shown in the inset of figure IX) will expand and eventually encircle the minus one point once. This indicates that increasing the gain will only add to the instability by putting another pole in the right half plane. The Nyquist plot at a speed of 4 knots is not significantly different to change the results regarding stability.

To add to the sophistication of the control system by includ- yaw rate feedback in the system, we can most easily visualize the stability problem by a root locus plot. The determination of the exact breakaway point requires the solution of a sixth degree equation, but the trend of the system can be seen without the exact solution. The poles and zeros of the open loop transfer function and the asymptotes for speed of 4 and 7.5 knots are plotted in figures X and XI. The effect of proportional plus first derivative control is to add another zero to the plot and its position would be governed by the ratio of the gains of the proportional to the first derivative terms. With the total

FIGURE IX

Nyquist Criteria-Plot

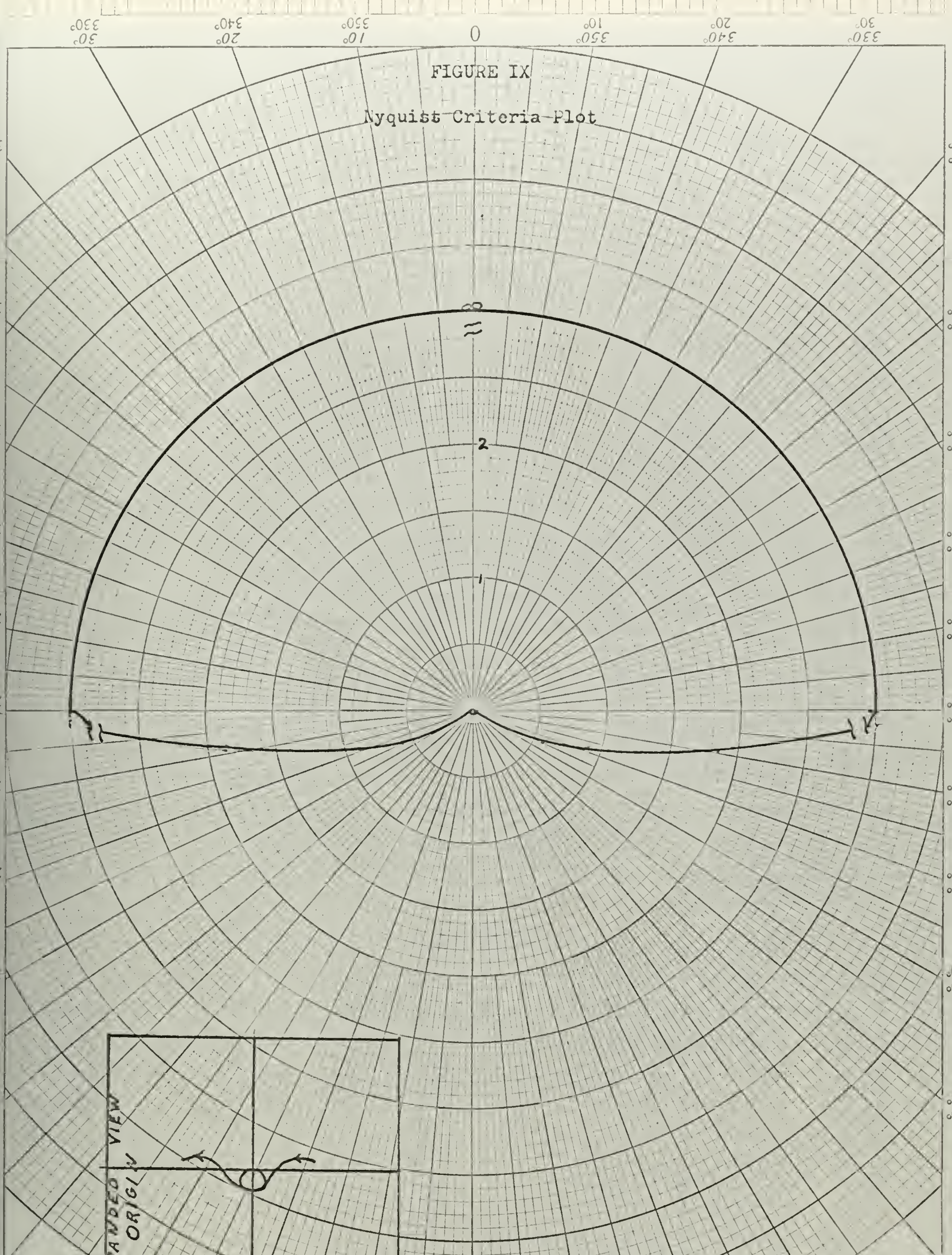

Root locus with 4.5 Knots

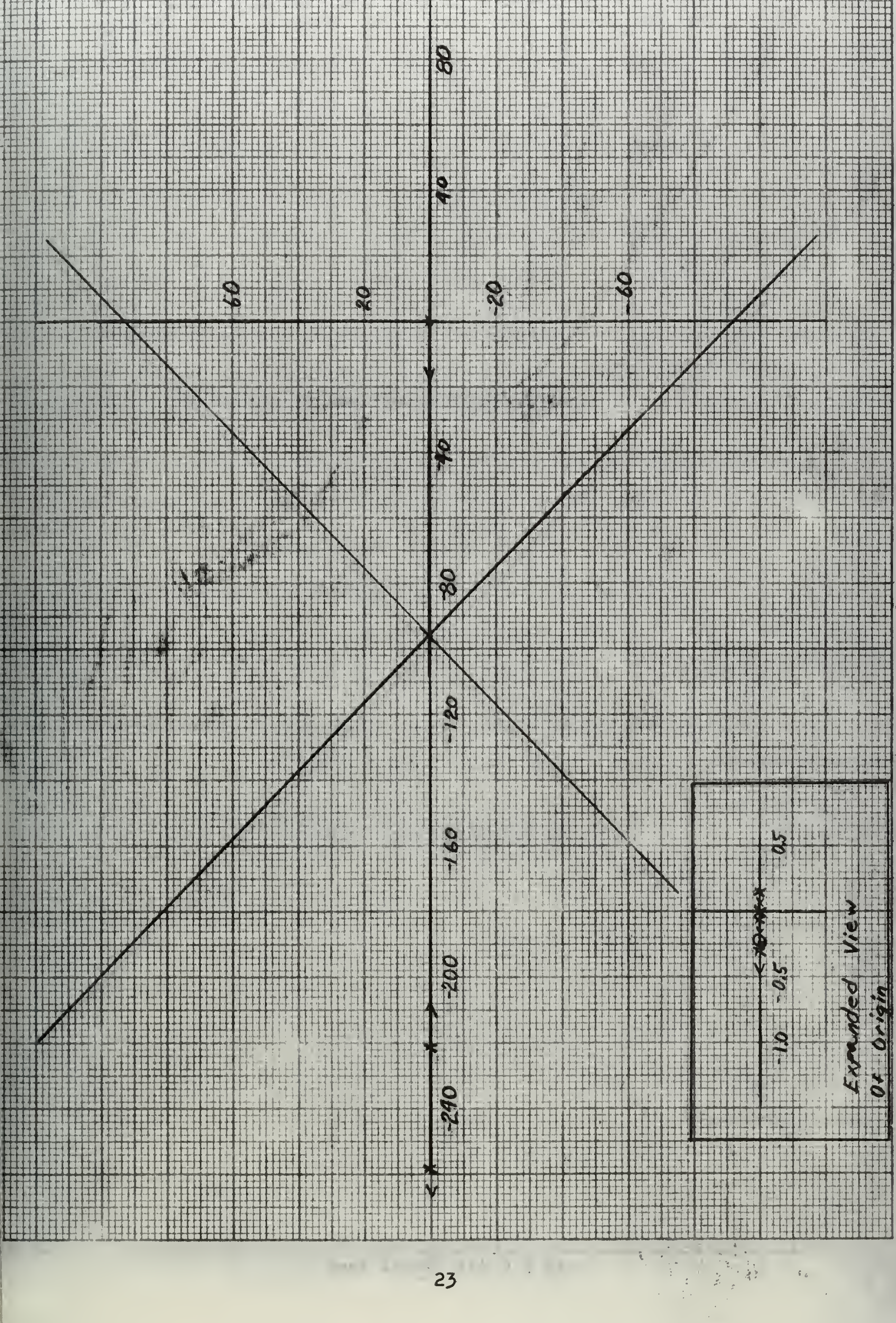

Root Locus at 7.5 Knots

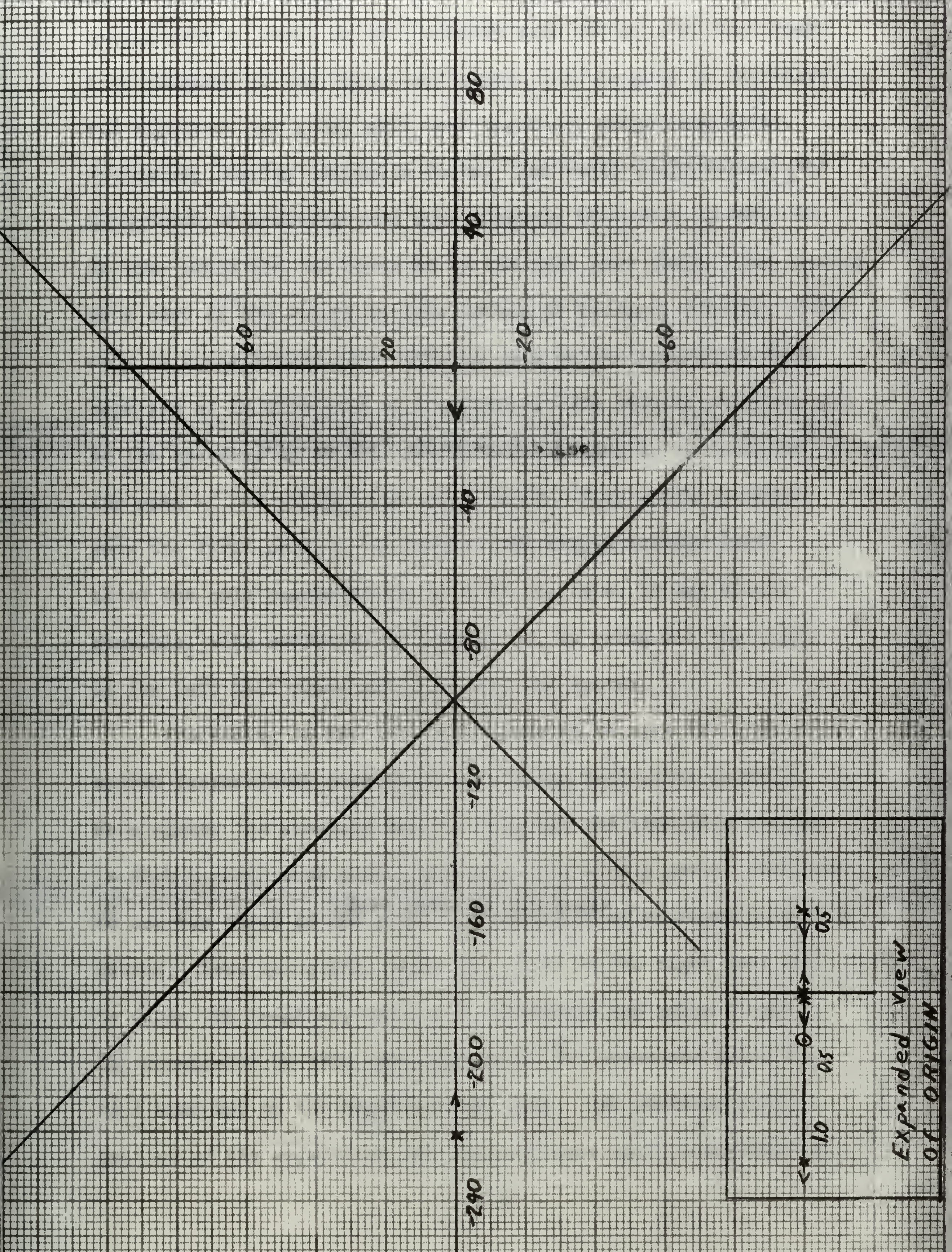

system gain at zero, we will already have one pole of the closed loop transfer in the right half plane. As the gain is increased, the rightmost two poles will come together, merge, and split, indicating complex conjugate roots. The roots would follow ±45° asymptotes originating from approximately the -95.9 point. At no time would all the roots be in the left half plane. The placing of a zero at the origin by this method of feedback control, could only be accomplished with infinite gain on the derivative feedback and so is dismissed as a solution. The only alternative will be the speeding up of the control system, such as by reducing the mass of the plunger and spool valve. This would in effect move the first pole on the left of the origin further left. After the pole passes to the left of the zero, it may become possible, with sufficiently high gains, to bring all the roots to the left half plane and stabilize the system.

Proceeding to the next step would be to make the control system proportional plus first and second derivative control. Here again, the simplest way to visualize the stability problem is with a root locus plot. The effect of such a system would be to add two zeros to the plot. By selection of appropriate gain ratios, these zeros will cause the poles on the right half plane to cross the imaginary axis at a relatively low value of gain. The asymptotes in this case will be at 60° above and below the real axis and on the negative real axis. The point of intersection of the asymptotes and the real axis will be governed by the

real part of the position of the two new zeros. The 60° slopes obviously indicates that excessive gain will again place the roots in the right half plane and unstabilize the system. As was mentioned before, systems with second derivative feedback have not proved satisfactory for automatic steering control aboard ship. The control system tends to produce relatively high frequency oscillations of the steering device. A continual movement of the steering control would be necessary to stabilize a dynamically unstable ship, but these systems tend to cause much more motion than is needed for effective control. The introduction of a second degree lag network into the control system is recommended by Rydill (3) to help reduce these oscillations.

CONCLUSION

It is evident that any attempt at automatic control for yaw stabilization of an LCVP without a skeg, will be difficult and uneconomical. By using the skeg to restore dynamic stability to the craft before the control system is added, a great deal of complexity will be eliminated. The dynamically stable craft will naturally be easier to handle when steering manually. The use of pump jet propulsion appears to be a practical method of propelling and controlling landing craft and is adaptable to automatic control.

RECOMMENDATIONS

The most important recommendation can only be to use a skeg to make the LCVP dynamically stable to begin with. If this scheme of testing is to be used again for this model, Jacob's method may be used to include the use of the skeg too.

The testing in the towing tank should include some means of obtaining resistance data while in a surf. This will govern the thrust available for control. I suggest that some ramp be installed in the tank near the wave maker to generate breakers. This ramp would have the same effect as a reef in causing the waves to become breakers. I feel any attempts to gather data using waves breaking on the tank's beach will prove futile, due to the short length of surf.

BIBLIOGRAPHY

1. Abkowitz, M. A., Lectures on Ship Hydrodynamics-Steering and Maneuverability, Danish Technical Press, May 1964.

2. Jacobs, W. R., Estimation of Stability Derivatives and Indices of Various Ship Forms, and Comparison with Experimental Results, Davidson Laboratory Report 1035, September, 1964.

3. Rydill, L. J., A Linear Theory for the Steered Motion of Ships in Waves, Transaction of the Institution of Naval Architects, Vol. 101, 1959, pp. 81-112.

4. Schiff, L. J. and Gimpirch, M., Automatic Steering of Ships by Proportional Control, Society of Naval Architects and Marine Engineers Transactions, Vol. 57, 1949, pp. 94-124.

APPENDIX

APPENDIX A

The following is a brief description of the Jacobs' (2) method of determining stability indices. The first step was to determine the sectional inertia coefficients C_s by entering figure XVII with the values of sectional area divided by local beam times local draft ($\frac{A}{bh}$) and local beam divided by local draft ($\frac{b}{h}$). Next, Lamb's coefficients of accession to inertia (k_1, k_2, k') are found from figure XVIII by entering with $\frac{2h}{m_1}$. The prime in the following equations will denote non-dementionalized quantities. (note all quantities here are non-dementionalized by the quantities noted in the chapter on results) The limits on the integrals $x_b + x_s$ represent bow to stern.

$$m_2 = k_2 \frac{\rho}{2} \int_{x_s}^{x_b} C_s h^2 \, dx \qquad (4)$$

$$m_2' = \frac{m_2}{\frac{\rho}{2} l^2 h_m} \qquad (5)$$

$$I_y' = \frac{h_m}{l} \qquad (6)$$

$$m_z' = \frac{k'}{k_2} m_2' \qquad (7)$$

$$\bar{x} = \frac{\int_{x_s}^{x_b} C_s h^2 x \, dx}{\int_{x_s}^{x_b} C_s h^2 \, dx} \qquad (8)$$

$\frac{x}{l}$ = half the prismatic coefficient (9)

$$N_{\dot{r}} = k' \frac{\pi \rho}{2} \int_{x_s}^{x_b} C_s h^2 x^2 dx \tag{10}$$

$$Y_{\dot{r}} = m_1 = k_1 m_o \tag{11}$$

$$Y_{\dot{r}} = -m_2 \bar{x} \tag{12}$$

$$N_{\dot{r}} = -m_2 \bar{x} \tag{13}$$

$$Y'_r = -(m'_o + m'_1) - \frac{x_p}{l} L'_\psi \tag{14}$$

$$Y_r = Y'_r \frac{\rho}{2} uhl \tag{15}$$

$$N'_r = -m'_z \frac{\bar{x}}{l} \left(\frac{x_o}{l}\right)^2 L'\psi \tag{16}$$

$$N_r = N'_r \frac{\rho}{2} uhl^2 \tag{17}$$

Figures XII through XVI are the calculations required to derive these stability derivatives and indices for the LCVP tested. The integrations were carried out by Simpson's rule and all areas found by use of a planimeter.

FIGURE XII

Station	h^2	C_s	$C_s h^2$	Lever	S.M.	$\int C_s h^2 dx$	$\int C_s h^2 x dx$
0	0	0	0	0	1	0	0
2	0	0	0	0	4	0	0
4	1.32	0.85	1.122	14.91	2	2.244	33.5
6	3.33	0.87	2.9	12.41	4	11.6	144.0
8	4.68	0.88	4.12	9.91	2	8.23	81.6
10	5.10	0.90	4.59	7.41	4	18.38	136.2
12	5.13	0.97	4.98	4.91	2	9.96	49.0
14	4.60	1.03	4.74	2.41	4	18.97	45.7
16	4.00	1.02	4.08	-0.09	2	8.16	-0.73
18	3.27	1.09	3.56	-2.59	4	14.25	-36.9
20	3.15	1.06	3.34	-5.09	2	6.68	-34.0
22	3.20	1.06	3.39	-7.59	4	13.58	-103.0
24	3.20	1.03	3.29	-10.09	2	6.58	-66.4
26	3.30	0.96	3.17	-12.59	4	12.7	-159.5
28	3.50	0.97	3.40	-15.09	1	3.40	-51.3
						134.73	38.17

$$\bar{x} = \frac{\int_{x_s}^{x_b} C_s h^2 x dx}{\int_{x_s}^{x_b} C_s h^2 dx} = \frac{38.17}{134.73} = 0.2835$$

$$m_2 = h_2 \frac{\rho}{2} \pi \int_{x_s}^{x_b} C_s h^2 dx = 0.935 \times \frac{1.99}{2} \pi \times 134.73 = 393.5$$

FIGURE XII (continued)

$$Y_{\dot{r}}=k_2\frac{\rho}{2}\int_{x_s}^{x_b}C_s h^2 x\,dx=0.935 \times 0.995 \times 3.14159 \times 38.17=111.5$$

$$N_{\dot{y}}=m_2\bar{x}=111.5$$

FIGURE XIII

Station	h	S.M.	F(Area)	Lever	F(Moment)
0	0	1	0	7	0
2	0	4	0	6	0
4	1.15	2	2.30	5	11.50
6	1.83	4	7.33	4	29.32
8	2.17	2	4.34	3	13.02
10	2.25	4	9.00	2	18.00
12	2.27	2	4.54	1	4.54
14	2.15	4	8.6	0	0
16	2.00	2	4.00	-1	-4.00
18	1.81	4	7.24	-2	-14.44
20	1.78	2	3.56	-3	-10.68
22	1.79	4	7.16	-4	-28.64
24	1.79	2	3.58	-5	-17.90
26	1.82	4	7.28	-6	-43.68
28	1.88	1	1.88	-7	-13.16
			70.86		-56.06

$$x_c = \frac{F(M)}{F(a)} \times 2.5 = \frac{56.06}{70.86} \times 2.5 = 1.98$$

$$m_0 = \frac{23,000}{32.2} = 7.14 \times 10^2 \text{ slugs}$$

$$m_a = \frac{714}{7.99 \times 32.367^2 \times 2.\text{[illegible]}} = \frac{714}{(1.995)(2.27)(1.043 \times 10^3)} = 3.03 \times 10^{-1}$$

$$L\gamma = \frac{\pi h_m}{l} = \frac{\pi 2.27}{32.367} = 2.205 \times 10^{-1}$$

$$m'_1 = k_1 m'_o = (0.035)(3.03 \times 10^{-1}) = 1.06 \times 10^{-2}$$

$$m'_z = \frac{k'}{k_2} m'_2 = \frac{0.813}{0.935} \times 1.67 \times 10^{-1} = 1.452 \times 10^{-1}$$

$$\bar{x} = 0.2835$$

$$\frac{x_o}{l} = \tfrac{1}{2} \frac{\overset{23{,}000}{2240} \times 35}{32.367 \times 15.6} = \tfrac{1}{2} \frac{359}{504} = 0.356$$

FIGURE XIV

Station	Area	S.M.	F(vol.)	Lever	F(moment)
0	0	1	0	7	0
2	0	4	0	6	0
4	3.84	2	7.78	5	88.90
6	8.06	4	32.24	4	128.96
8	10.85	2	21.70	3	65.10
10	12.83	4	51.32	2	102.64
12	14.75	2	29.50	1	29.50
14	15.60	4	62.40	0	0
16	13.88	2	27.76	-1	-27.76
18	13.50	4	54.00	-2	-108.00
20	12.32	2	24.64	-3	-73.92
22	12.12	4	48.48	-4	-193.92
24	11.32	2	22.64	-5	-133.20
26	10.12	4	40.48	-6	-242.88
28	10.28	1	10.28	-7	-71.96
			433.22		-416.54

$LCB=\frac{F(M)}{F(V)} \times 30=\frac{-416.54}{433.22} \times 30=-28.9$ inches aft

$\Delta=F(V)\frac{30}{12 \times 3}=433.22 \times \frac{2.5}{3}=360$ feet^3

[illegible]

[illegible]	[illegible]	[illegible]	[illegible]	[illegible]	[illegible]
	[illegible]	[illegible]		[illegible]	[illegible]
	[illegible]	[illegible]	[illegible]	[illegible]	[illegible]
[illegible]	[illegible]	[illegible]	[illegible]	[illegible]	[illegible]
[illegible]	[illegible]	[illegible]	[illegible]	[illegible]	[illegible]
[illegible]		[illegible]	[illegible]	[illegible]	[illegible]
[illegible]	[illegible]	[illegible]	[illegible]	[illegible]	[illegible]
[illegible]		[illegible]	[illegible]	[illegible]	[illegible]
[illegible]	[illegible]	[illegible]	[illegible]	[illegible]	[illegible]
[illegible]	[illegible]	[illegible]	[illegible]	[illegible]	[illegible]
[illegible]	[illegible]	[illegible]	[illegible]	[illegible]	[illegible]
[illegible]	[illegible]	[illegible]	[illegible]	[illegible]	[illegible]
[illegible]	[illegible]	[illegible]	[illegible]	[illegible]	[illegible]
[illegible]	[illegible]	[illegible]	[illegible]	[illegible]	[illegible]
[illegible]	[illegible]	[illegible]	[illegible]	[illegible]	[illegible]
[illegible]	[illegible]	[illegible]	[illegible]	[illegible]	[illegible]
[illegible]		[illegible]			

[illegible]

[illegible]

[illegible]

FIGURE XV

Station	Draft	h^2	Beam	Area	$\frac{b}{h}$	bh	Area_{bh}	C_s
0	0	0	0	0	0	0	0	0
2	0	0	0	0	0	0	0	0
4	1.15	1.32	7.17	3.89	6.24	8.25	.472	.85
6	1.825	3.33	7.82	8.06	4.29	14.28	.565	.87
8	2.167	4.68	8.15	10.85	3.76	17.72	.612	.88
10	2.260	5.10	8.48	12.83	3.76	19.20	.668	.90
12	2.27	5.13	8.67	14.75	3.82	19.68	.75	.97
14	2.15	4.6	8.75	15.6	4.07	18.8	.83	1.03
16	2.00	4.00	8.54	1388	4.27	1708	.813	1.02
18	1.81	3.27	8.38	13.5	4.63	15.18	.89	1.09
20	1.775	3.15	8.27	12.32	4.68	14.7	.84	1.06
22	1.70	3.20	8.10	12.12	4.52	14.5	.84	1.06
24	1.79	3.20	7.82	11.32	4.37	14.0	.81	1.03
26	1.82	3.30	7.53	10.12	4.14	13.7	.74	.96
28	1.875	3.50	7.23	10.28	3.86	13.58	.758	.97

minor axis major axis $= \frac{2h_m}{l} = \frac{4.54}{32.367} = 0.1402$

k'=0.813 (rotational)

k'=0.035 (longitudinal)

k_2=0.935 (lateral)

FIGURE XVI

Station	x	x^2	$C_s h^2$	$x^2 C_s h^2$	S.M.	$C_s h^2 x^2 dx$
0	0	0	0	0	1	0
2	0	0	0	0	4	0
4	14.91	222	1.122	249	2	498
6	12.41	154	2.9	447	4	1788
8	9.91	98	4.12	404	2	808
10	7.41	55	4.59	252	4	1008
12	4.91	24	4.98	119.5	2	239
14	2.41	5.8	4.74	27.5	4	110
16	-0.07	.0081	4.08	.03	2	.06
18	-2.59	6.7	3.56	23.8	4	95.2
20	-5.09	25.8	3.34	86.2	2	172.4
22	-7.59	57.3	3.39	194	4	776
24	-10.09	101.5	3.29	334	2	668
26	-12.59	158	3.17	500	4	2000
28	-15.09	227	3.40	771	1	771
						8933

$$8933 \times \frac{2.5}{3} = 7443 = \int_{xs}^{xb} C_s h^2 x^2 dx$$

$$N_r = 0.813 \times \frac{1.9905}{2} \times 7443 = 18{,}890$$

$$I = 7.14 \times 65.4 \times 10^2 = 46{,}700$$

FIGURE VII

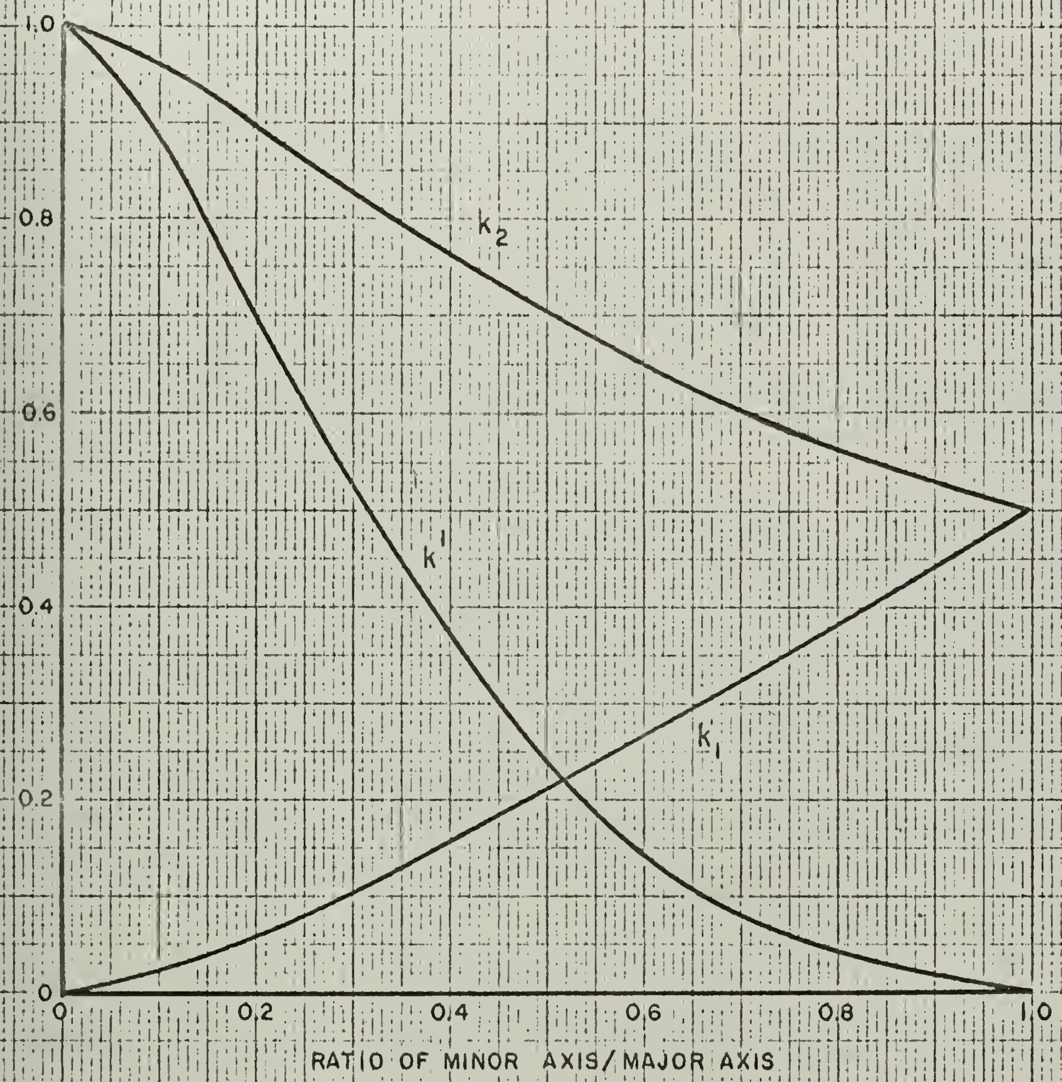

FIGURE 2. COEFFICIENTS OF ACCESSION TO INERTIA FOR PROLATE SPHEROIDS (FROM H. LAMB'S HYDRODYNAMICS)

FIGURE VIII

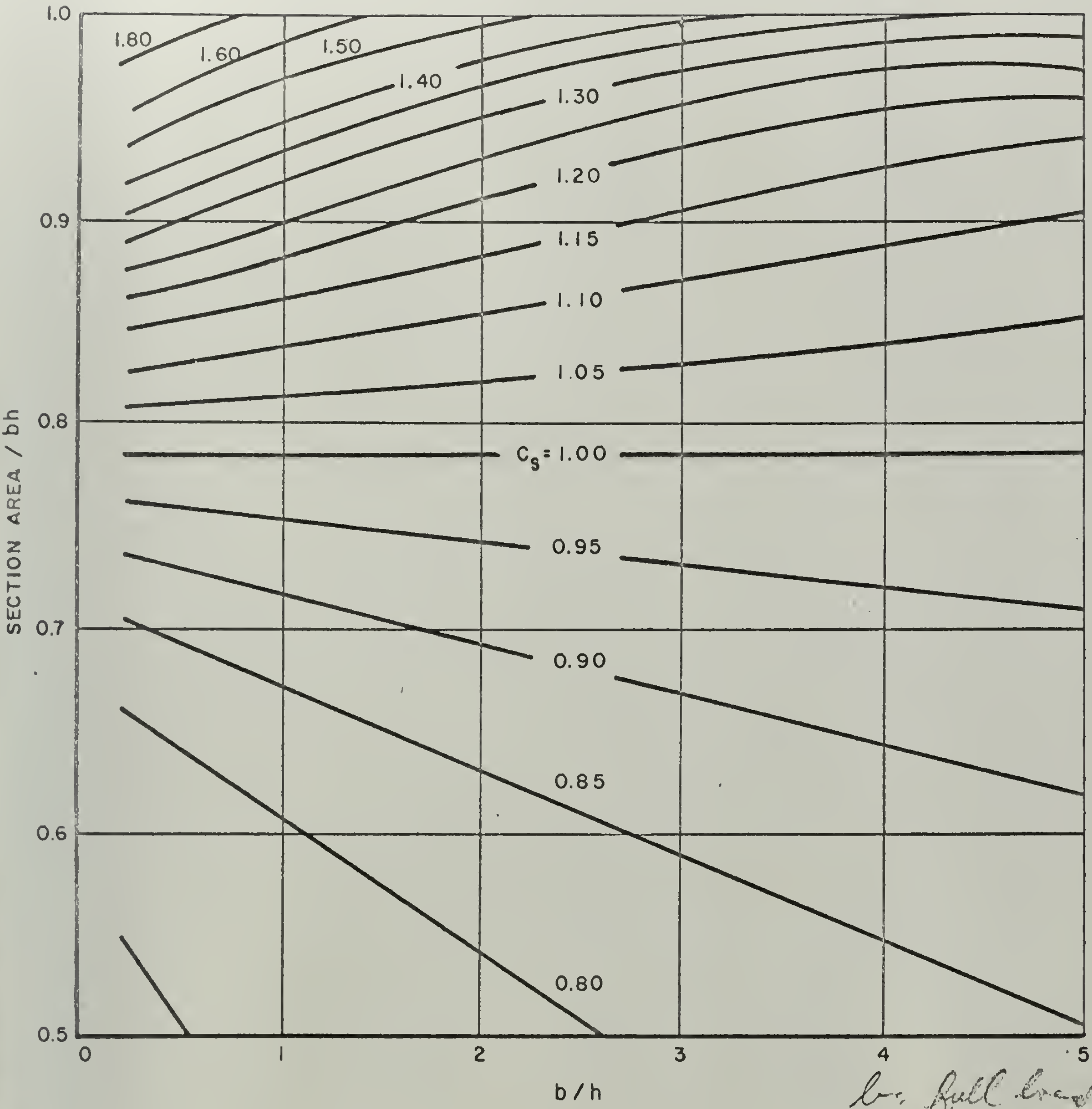

b = full load beam
h = load draft

SECTIONAL INERTIA COEFFICIENTS C_s AS FUNCTIONS OF THE LOCAL BEAM-DRAFT RATIO b/h AND SECTION AREA COEFFICIENT, FROM PROHASKA